Macromolecules
ARTICLE

Macromolecules **2009**, *42*, 8801–8808 **8801**
DOI: 10.1021/ma9017907

Prediction of the Ionic Liquid Influence on Propagation Rate Coefficients in Methyl Methacrylate Radical Polymerizations Based on Kamlet−Taft Solvatochromic Parameters

Aleksandra Jeličić,[†] Nuria García,[‡] Hans-Gerd Löhmannsröben,[†] and Sabine Beuermann*,[†]

[†]*Institute of Chemistry, University of Potsdam, Karl-Liebknecht Str. 24-25, 14476 Golm, Germany, and*
[‡]*Instituto de Ciencia y Tecnología de Polímeros (CSIC), Juan de la Cierva 3, 28006 Madrid, Spain*

Received August 10, 2009; Revised Manuscript Received August 31, 2009

ABSTRACT: Pulsed laser initiated polymerizations of methyl methacrylate (MMA) in the presence of ionic liquids (ILs) resulted in a strong enhancement of the propagation rate coefficient, k_p, compared to the bulk system. To correlate the IL influence on MMA k_p with IL solvent properties, the Kamlet−Taft parameters α, β, and π^* of the ILs were derived. A correlation in the form of $\ln(k_p/k_{p,\text{bulk}}) = \ln(k_p/k_{p,\text{bulk}})^0 + s\pi^* + a\alpha + b\beta$ was obtained from a linear solvation energy relationship (LSER) analysis of a data set consisting of polymerizations in 11 ILs, as well as in DMSO, in THF, and in bulk. The coefficients are $s = 1.72$, $a = 0.63$, $b = 0.37$, and $\ln(k_p/k_{p,\text{bulk}})^0 = -1.27$. The data indicate that dipolarity, polarizability, and electron pair accepting ability of the IL, associated with the π^* parameter, contribute to a large extent to the variation in k_p, whereas electron pair donating and hydrogen bond accepting ability, accounted for by β, are of lesser importance. The hydrogen bond donating ability, related to α, of the IL has no significant influence on k_p.

Introduction

The ability of ILs to dissolve a wide range of organic and inorganic compounds, their ionic nature, and their ability to undergo numerous solvent−solute interactions make them an interesting medium for various reactions.[1] Furthermore, due to environmental concerns, there is an increasing requirement to replace volatile organic compounds (VOC). Thus, because of their generally negligible vapor pressure, ILs are considered as attractive replacements for VOCs.

ILs have already been used as reaction media for numerous chemical synthesis. Of particular interest are cases where the presence of ILs increases yield, rate of reaction, and selectivity or significantly facilitates product separation due to different solubilization of catalysts, reagents, and products.[1] IL applications in polymer science are investigated for about a decade. In addition to being used as a novel polymerization medium, ILs were employed, e.g., for the preparation of functional polymers, as components of polymer matrices or gels, or as templates for porous polymers.[2−8]

Investigations into radical polymerizations in ILs revealed significant changes in polymerization rates and molecular weights when compared to conventional solvents.[9−14] In particular, propagation rate coefficients, k_p, of MMA in ILs obtained from pulsed laser initiated polymerizations (PLP) with subsequent polymer analysis via size-exclusion chromatography (SEC) showed a k_p enhancement in all cases. For example, MMA k_p in [EMIM][EtSO$_4$][12] and [HMIM]Cl[14] is 4 times as high as the associated bulk value. Because of the high viscosity of ILs, the diffusion-controlled MMA termination rate coefficients were reported to decrease by an order of magnitude.[11] In a homologous series of ILs MMA k_p increases as the size of cation and/or anion decreases.[14] Polarity was suggested to be the most probable origin of the k_p enhancement observed.[11−14] Further, ILs were found to influence the monomer reactivity ratios in free-radical copolymerizations.[15−18]

Nowadays, ILs of widely differing physicochemical properties are available. Bearing in mind the ability of ILs to significantly influence radical polymerization kinetics, ILs may be considered as "designer solvents". However, such a successful utilization of ILs requires a detailed understanding of the origin of the IL influence on polymerization rate coefficients. Ideally, the IL influence should be expressed by a mathematical correlation of the rate coefficients with IL-specific physicochemical parameters allowing for a prediction of individual rate coefficients for polymerizations in ILs.

Previous attempts to correlate MMA k_p for polymerizations in ILs with normalized polarity values, E_T^N, of the ILs only allowed for a rough estimate of k_p. It was concluded that a more rigorous approach has to be applied to account for polarity effects.[14] Such an approach is Kamlet−Taft's linear solvation energy relationship (LSER).[19] While E_T^N values are representative of both nonspecific dye/solvent interactions and specific Lewis acid/base interactions, the LSER breaks down polarity into dipolarity and polarizability, hydrogen bond donating (HBD) acidity, and hydrogen bond accepting (HBA) basicity. Generally, LSER is used to identify and quantify the individual solute−solvent interactions that determine the solvent effect on a particular physicochemical property or kinetic data. One of the most common forms of the Kamlet−Taft LSER is given by eq 1:[19]

$$XYZ = XYZ^0 + s(\pi^* + d\boldsymbol{\delta}) + a\alpha + b\beta \qquad (1)$$

where XYZ represents a solvent-dependent physicochemical property or reactivity parameter in a given solvent. XYZ^0 represents XYZ under gas phase conditions or in an inert solvent. β is a measure of HBA basicity of a solvent or its ability to accept a hydrogen bond. Moreover, β is a measure of the electron-pair donating (EPD) ability of solvents. π^* represents the solvent dipolarity/polarizability, which measures the ability of a solvent

---

*Corresponding author. E-mail: sabine.beuermann@uni-potsdam.de.

to stabilize a neighboring charge or a dipole by virtue of nonspecific dielectric interactions. If a set of data for a number of solvents with considerably different polarizabilities is analyzed by LSER, a polarizability correction term, δ, is preferably used. For aromatic solvents $\delta = 1.00$, for polychlorinated aliphatic solvents $\delta = 0.50$, and for all other aliphatic solvents $\delta = 0.00$ were reported.[20] The electron-pair accepting (EPA) ability of a solvent, as one of the potential interactions of interest with ILs, is accounted for by π^*. The α parameter is associated with the ability to donate a hydrogen for H bonding (HBD). a, b, s, and d are coefficients that describe the sensitivity of XYZ toward α, β, π^*, and δ. It should be noted that XYZ^0, a, b, s, and d are solvent-independent coefficients, which are derived from a multiparameter fit to a number of solvent-dependent observations and which are characteristic for the process under investigation.

LSER analyses were already successfully applied to understand solvent effects on many types of physicochemical properties and reactivity parameters in organic reactions.[19,21–27] The use of LSER does not only provide information on relative contributions of each parameter; moreover, the sign of the coefficients a, b, s, and d indicates whether the reactants or the transition state is preferably stabilized by the solvent.[21,25,27–29] First attempts to apply LSER to understand the solvent influence on propagation rate coefficients by Czerwinski suffered from the fact that at that time reliable PLP-SEC derived rate coefficients were only scarce.[30] Moreover, the solvent induced variations in k_p were rather low.

In this publication, MMA k_p data for polymerizations in ILs are correlated with IL or MMA/IL solvatochromic parameters applying the LSER approach. To extend the existing data set,[14] k_p data for polymerizations in 1-ethyl-3-methylimidazolium *n*-hexylsulfate, 1-butyl-3-methylimidazolium tetrafluoroborate and hexafluorophosphate, and 1-hexyl-3-methylimidazolium hexafluorophosphate and bromide were determined.

Experimental Section

Materials. Methyl methacrylate (MMA, Aldrich, 99%), the photoinitiator 2-methyl-4′-(methylthio)-2-morpholinopropiophenone (MMMP, Aldrich, 98%), the solvatochromic dyes 2,6-diphenyl-4-(2,4,6-triphenyl-1-pyridinio)phenolate (Reichardt's dye, Fluka, techn ≥90%), *N*,*N*-diethyl-4-nitroaniline (Fluorochem, 97%), and 4-nitroaniline (Aldrich, ≥99%), dimethyl sulfoxide (DMSO, Roth, ≥99%), and the ionic liquids 1-hexyl-3-methylimidazolium chloride ([HMIM]Cl, Solvent Innovation, 98%), 1-butyl-3-methylimidazolium *n*-octylsulfate ([BMIM][OctSO$_4$], Fluka, ≥95%), trioctylmethylammonium bis(trifluoromethylsulfonyl)imide ([OMA][Tf$_2$N], IoLiTec, 99%), 3-methyl-1-octylpyridinium tetrafluoroborate ([MOPYR][BF$_4$], Solvent Innovation, 99%), 1-ethyl-3-methylimidazolium *n*-octylsulfate ([EMIM][OctSO$_4$], Solvent Innovation, 98%), 1-methyl-3-octylimidazolium tetrafluoroborate ([MOIM][BF$_4$], Solvent Innovation, 99%), 1-ethyl-3-methylimidazolium *n*-hexylsulfate ([EMIM][HexSO$_4$], Solvent Innovation, 98%), 1-hexyl-3-methylimidazolium hexafluorophosphate ([HMIM][PF$_6$], IoLiTec, 99%), 1-hexyl-3-methylimidazolium bromide ([HMIM]Br, IoLiTec, 98%), 1-butyl-3-methylimidazolium tetrafluoroborate ([BMIM][BF$_4$], IoLiTec, 99%), and 1-butyl-3-methylimidazolium hexafluorophosphate ([BMIM][PF$_6$], IoLiTec, 99%) were used as received. The ILs, THF, DMSO, and MMA were used as received for the UV measurements, since free radical polymerizations are generally very robust and do not require special purification of the components. Methanol (VWR, 99%) containing trace amounts of hydroquinone (Fluka, 98%) was used to precipitate the polymer. *N*,*N*-Dimethylacetamide (Acros, 99%) containing LiBr (Riedel-de Haen, 99%) was used as eluent for SEC.

Pulsed Laser Initiated Polymerization. Pulsed laser initiated polymerizations were carried out at 25 ± 2 °C using a thermostated cuvette (Hellma 165 QS, 10 mm path length). Experimental details are given in ref 14. As a representative reaction temperature, the arithmetic mean temperature, T, of the sequentially registered temperatures was considered. The difference between the initial and the final temperature during PLP ranges from 0.3 to 2.0 °C depending on IL type and concentration as well as on the initial temperature. The importance of monitoring the temperature during PLP was pointed out by García et al. previously.[31] MMA k_p bulk data from ref 31 were taken for comparison with the k_p values determined in this study as the majority of PLP experiments were conducted under the same experimental conditions as in ref 31.

Monomer−IL solutions with MMMP concentrations ranging from 0.5 to 7.1 mmol L^{-1} were prepared. Initiator decomposition was induced using a Q-switched Nd:YAG laser (B. M. Industries, 5000 series) operating at 355 nm with a repetition rate, ν_{rep}, of 5 Hz, a pulse energy, E_p, of ~6 mJ, and a pulse width in the range of 10 nm. The number of pulses was chosen such that the conversion of monomer did not exceed 10%. The polymer was precipitated in methanol containing traces of hydroquinone to prevent further polymerization, washed twice with methanol to remove the ionic liquid, and dried in vacuum prior to SEC analysis.

Size-Exclusion Chromatography. Molecular weight distributions (MWDs) were obtained by size exclusion chromatography using an Agilent 1200 isocratic pump, an Agilent 1200 refractive index detector, and three GRAM columns (8 × 300 mm, particle size 10 μm, pore sizes 100 and 2 × 3000 Å) from PSS. *N*,*N*-Dimethylacetamide containing 0.1% LiBr at 45 °C at a flow rate of 1 mL min^{-1} was used as eluent. The SEC setup was calibrated against PMMA standards of narrow polydispersity (MW between 500 and 1×10^6 g mol^{-1}, PSS).

UV/vis Measurements. Absorption spectra of the solvatochromic dyes dissolved in MMA, THF, DMSO, ILs, and in MMA/solvent mixtures were recorded on a Perkin-Elmer Lambda 750 absorption spectrometer. The spectra were recorded in Hellma QS quartz cuvettes with 1 mm path length in the wavelength range from 300 to 1000 nm at room temperature. The concentration of the solvatochromic dye was chosen to yield absorbances of the observed absorption bands in the range from 0.4 to 2.

As Reichardt's dye is sensitive to the presence of acid, a few microliters of triethylamine were added to [EMIM][HexSO$_4$], [HMIM]Cl, [HMIM]Br, and [BMIM][BF$_4$] to scavenge acid that may protonate the phenoxide form.[32] Control experiments showed that even addition of 5 wt % of triethylamine did not shift the absorption maximum in the above-mentioned ILs.

Random samples were chosen to check for reproducibility of UV/vis measurements. Based on the spectroscopic data, mean absolute deviations for π^*, α, and β were calculated to be at most ±0.02 and for E_T^N ±0.01.

Results and Discussion

To gain a better understanding of MMA k_p enhancement due to the presence of ILs and to obtain the most reliable LSERs, the existing data set from ref 14 was extended by the determination of MMA k_p at ~26 °C in DMSO, [EMIM][HexSO$_4$], [BMIM][BF$_4$], [BMIM][PF$_6$], [HMIM]Br, and [HMIM][PF$_6$] for concentrations between 2.11 and 2.16 mol L^{-1}. To investigate the influence of IL concentration on the propagation kinetics, additionally MMA k_p values for polymerizations in [HMIM][PF$_6$] were estimated for c_M ranging from 2 to 7 mol L^{-1} at $T \sim 26$ °C. Note that previously determined k_p values in the before-mentioned solvents refer to different c_M or temperatures. As $k_p/k_{p,\text{bulk}}$ varies with monomer concentration and the activation energy of k_p is affected by the presence of ILs, only MMA k_p obtained under ostensibly the same experimental conditions were considered here.

MMA k_p was derived applying the PLP-SEC technique developed by Olaj and co-workers,[33] which was recommended as the

Table 1. Experimental Details (Monomer Concentration, c_{M}, Photoinitiator Concentration, c_{MMMP}, Temperature, T, and Molecular Weights at the First and Second Inflection Point, M_1 and M_2, Respectively), Propagation Rate Coefficient, k_{p}, and $k_{\mathrm{p}}/k_{\mathrm{p,bulk}}$ ($k_{\mathrm{p,bulk}}$ Being the Rate Coefficient for Bulk Reactions) for Polymerizations in the Indicated Solvents[a]

solvent	c_{M}/mol L^{-1}	c_{MMMP}/mmol L^{-1}	T/°C	M_1/g mol^{-1}	M_2/g mol^{-1}	M_1/M_2	k_{p}/L mol^{-1} s^{-1}	$k_{\mathrm{p}}/k_{\mathrm{p,bulk}}$
DMSO	2.14	0.5	25.8	28 400	55 500	0.51	662	2.2
DMSO	2.13	2.0	26.1	27 000	55 200	0.49	631	2.1
DMSO	2.13	2.0	26.0	27 400	56 300	0.49	642	2.1
[EMIM][HexSO$_4$]	2.14	0.5	26.2	33 400	67 500	0.49	779	2.6
[EMIM][HexSO$_4$]	2.14	0.5	26.3	33 900	66 800	0.51	790	2.6
[BMIM][BF$_4$]	2.11	2.2	25.2	40 700	80 100	0.51	965	3.3
[BMIM][BF$_4$]	2.11	2.2	25.4	41 800	79 300	0.53	992	3.4
[BMIM][PF$_6$]	2.14	2.2	26.4	38 600	76 600	0.50	900	2.9
[BMIM][PF$_6$]	2.14	2.2	26.4	38 800	76 500	0.51	904	3.0
[HMIM]Br	2.14	1.6	25.6	44 700	92 500	0.48	1041	3.5
[HMIM]Br	2.14	1.6	25.6	43 900	94 200	0.47	1023	3.4
[HMIM][PF$_6$]	2.16	2.2	25.9	32 600	65 000	0.50	755	2.5
[HMIM][PF$_6$]	2.16	2.2	26.0	33 100	66 000	0.50	766	2.5
[HMIM][PF$_6$]	3.23	3.2	25.4	42 000	84 300	0.50	650	2.2
[HMIM][PF$_6$]	3.23	3.2	25.0	41 700	83 500	0.50	645	2.2
[HMIM][PF$_6$]	5.07	5.1	25.0	52 000	108 000	0.48	513	1.8
[HMIM][PF$_6$]	5.07	5.1	25.1	52 800	108 000	0.49	521	1.8
[HMIM][PF$_6$]	7.07	7.1	25.1	55 700	116 000	0.48	393	1.3
[HMIM][PF$_6$]	7.07	7.1	25.8	57 700	121 000	0.48	408	1.4

[a] Pulse repetition rate: 5 Hz; laser pulse energy: 6 mJ.

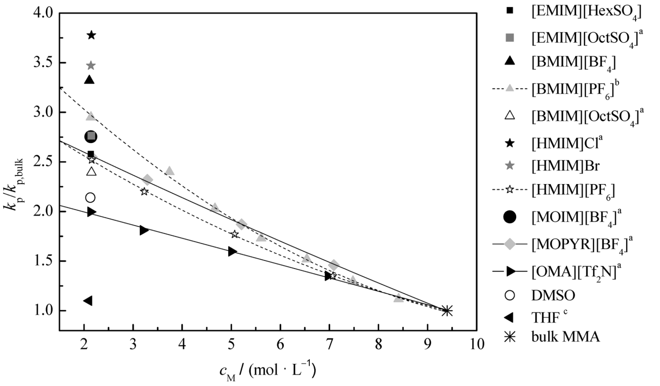

Figure 1. Propagation rate coefficients, k_{p}, for MMA polymerizations in ILs, DMSO at 25 ± 2 °C, and THF at 40 °C relative to the bulk rate coefficient, $k_{\mathrm{p,bulk}}$, vs monomer concentration, c_{M}: (a) ref 14; (b) combined data set from ref 11 and from this work; (c) ref 38.

method of choice for the determination of k_{p} by the IUPAC Working Party on *Modeling of Polymerization Kinetics and Processes*.[34] k_{p} is calculated according to eq 2:

$$L_1 = k_{\mathrm{p}} c_{\mathrm{M}} t_0 \qquad (2)$$

where c_{M} is the monomer concentration, t_0 the time between two successive laser pulses, and L_1 the number of propagation steps between two pulses. L_1 is calculated as M_1/M_{MMA}, where M_{MMA} is the molar mass of the monomer and M_1 may be identified by the first inflection point of the molecular weight distribution (MWD).[33,35] To derive reliable k_{p} values, the existence of a second or even a third inflection point at degrees of polymerization around $L_2 = 2L_1$ and $L_3 = 3L_1$ is required. These higher order inflection points serve as a consistency criterion for k_{p} determination via PLP−SEC.[36,37] Details of each experiment and associated k_{p} values are listed in Table 1. In all cases the ratio M_1/M_2 is close to 0.5, indicating that the PLP consistency criterion is fulfilled. The data for duplicate experiments in Table 1 demonstrate excellent reproducibility with deviations being smaller than 5% for experiments at ostensibly the same conditions.

In Figure 1, MMA k_{p} for polymerizations in ILs from this work and from refs 11 and14 are plotted as a function of c_{M}. Further, MMA k_{p} values for polymerizations in DMSO and THF[38] are contained. All data are given relative to the corresponding bulk value. All $k_{\mathrm{p}}/k_{\mathrm{p,bulk}}$ refer to 25 ± 2 °C, with the exception of k_{p} from polymerizations in THF, which were carried out at 40 °C.[38] To use the latter data is justified because the activation energies of k_{p} for polymerizations in THF and in bulk are not significantly different.[38] For clarity of presentation, arithmetic mean values are given for each c_{M}.

Figure 1 demonstrates that k_{p} is increased by up to a factor of 2−4 due to the presence of ILs. For [HMIM][PF$_6$], [BMIM][PF$_6$], [OMA][Tf$_2$N], and [MOPYR][BF$_4$] the variation of k_{p} with c_{M} was studied in more detail.[11−14] While a linear dependence of k_{p} on c_{M} is found for polymerizations in [OMA][Tf$_2$N] and in [MOPYR][BF$_4$], a slightly curved dependence is found with [HMIM][PF$_6$] and [BMIM][PF$_6$]. For [HMIM]Cl, [HMIM]Br, and [BMIM][BF$_4$] resulting in the strongest enhancement of k_{p} the entire c_{M} range could not be studied due to homogeneity issues.

If analogous series of ILs with the same cation are considered, k_{p} changes in the following order: [BMIM][OctSO$_4$] < [BMIM][PF$_6$] < [BMIM][BF$_4$] and [HMIM][PF$_6$] < [HMIM]Br < [HMIM]Cl. In accordance with the findings from refs 12 and14 an increase in k_{p} is observed as the anion size decreases. k_{p} values for polymerizations in [EMIM][HexSO$_4$] and [EMIM][OctSO$_4$] deviate from this trend. Within experimental accuracy MMA k_{p} values for reactions in both ILs coincide. The reason may be seen in the rather small relative differences in size of the rather large hexyl and octyl sulfate anions. For ILs having the same anion the following order for the IL influence on k_{p} is found: [BMIM][OctSO$_4$] < [EMIM][OctSO$_4$], [MOPYR][BF$_4$] < [MOIM][BF$_4$] < [BMIM][BF$_4$], and [HMIM][PF$_6$] < [BMIM][PF$_6$]. As observed for the correlation of k_{p} with the anion size, the smaller the cation, the higher the associated k_{p} values. It is evident that MMA k_{p} is influenced by both anion and cation.

In previous PLP-SEC studies into the influence of supercritical carbon dioxide or organic solvents, e.g., toluene and THF, on methacrylate propagation kinetics the observed variation in k_{p} was assigned to the occurrence of local monomer concentrations rather than to a true kinetic effect.[38−40] This explanation was supported by the finding that the activation energies and activation volumes of k_{p} were not affected by the presence of the solvents. Moreover, the observed variations in k_{p} were comparably small; e.g., the largest variation in k_{p} due to the presence of supercritical carbon dioxide was 40%. In contrast, the variation in k_{p} observed here amount up to a factor of 4. Since the reaction mixtures stayed homogeneous and since the activation energies

Scheme 1. Structures of Solvatochromic Dyes Used for Calculating Solvatochromic Parameters: 4-Nitroaniline (1), *N,N*-Diethyl-4-nitroaniline (2), and Reichardt's Dye (3)

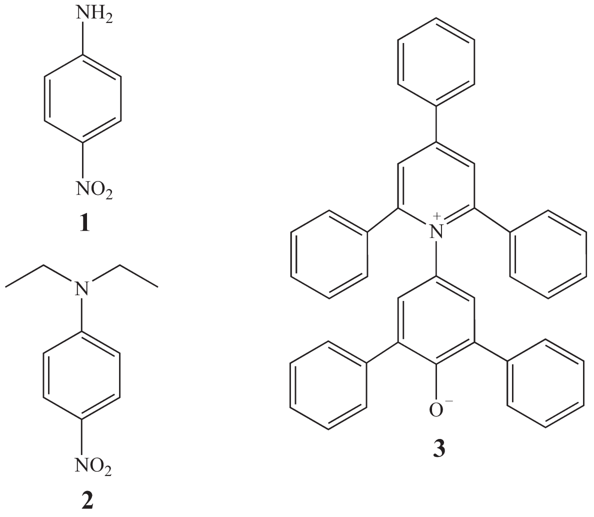

are affected by the presence of the ILs,[11,12,14] it appears highly unlikely that such a strong variation in monomer concentration throughout the reaction mixture occurs. Of course, the occurrence of local concentrations cannot be excluded completely. However, as discussed in more detail in ref 13, the contributions are considered to be negligible. To explain the IL-induced variation in k_p in the following the properties of the ILs will be considered.

Recently, it was shown that the IL influence on k_p cannot be predicted by E_T^N values of the pure ILs or mixtures of monomer and IL. It was concluded that the solvent influence is highly complex and involves both specific and nonspecific solvent−solute interactions.[14] To account for all these interactions Kamlet−Taft parameters were determined. In a number of studies several sets of dyes were used to determine a set of Kamlet−Taft parameters. Frequently, average values of these parameters were calculated. As the goal of this study is not only to understand experimentally obtained k_p values but also to identify a simple way to predict MMA k_p, the Kamlet−Taft parameters α, β, and π^* were derived from a single set of commercially available, commonly used solvatochromic dyes: Reichardt's dye, *N,N*-diethyl-4-nitroaniline, and 4-nitroaniline. The structures of these dyes are depicted in Scheme 1.

Representative of all systems, Figure 2 depicts UV/vis spectra of all three dyes in MMA and in [HMIM]Cl. For clarity of presentation, UV/vis spectra of Reichardt's dye in MMA and [HMIM]Cl are not shown below 450 nm to avoid overlapping with spectra of 4-nitroaniline and *N,N*-diethyl-4-nitroaniline, and because this spectral range is not used for derivation of the Kamlet−Taft parameters.[29] Figure 2 indicates that only a rather small shift of the absorption lines of 4-nitroaniline and *N,N*-diethyl-4-nitroaniline in MMA and in [HMIM]Cl occurs. Contrary, the absorption spectra of Reichardt's dye in MMA and in [HMIM]Cl are strongly different. The peak maximum of the absorption is shifted by 174 nm in [HMIM]Cl compared to MMA, pointing at remarkable differences in the ability of MMA and the ILs to undergo solute−solvent interactions with Reichardt's dye.

The Kamlet−Taft solvatochromic parameters are calculated on the basis of eqs 5−7. $E_T(30)$ values are obtained by measuring the wavelength corresponding to the maximum of the longest wavelength intramolecular $\pi-\pi^*$ absorption band of Reichardt's dye, $\lambda(3)_{\max}$.[41]

$$E_T(30)/(\text{kcal mol}^{-1}) = \frac{28591}{\lambda(3)_{\max}/\text{nm}} \qquad (3)$$

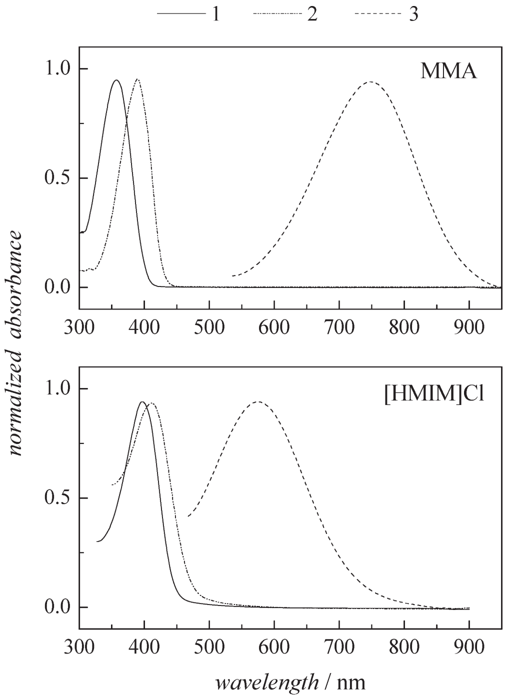

Figure 2. UV−vis absorption spectra of 4-nitroaniline (**1**), *N,N*-diethyl-4-nitroaniline (**2**), and Reichardt's dye (**3**) in MMA and in [HMIM]Cl.

$E_T(30)$ is the energy required to promote Reichardt's dye from the ground to the excited state. The normalized E_T^N polarity is calculated according to

$$E_T^N = \frac{E_T(30)/(\text{kcal mol}^{-1}) - 30.7}{32.4} \qquad (4)$$

The Kamlet−Taft parameter π^* is obtained by measuring the wavenumber at maximum absorbance, $\tilde{\nu}(2)_{\max}$, of *N,N*-diethyl-4-nitroaniline:[42]

$$\pi^* = \frac{\tilde{\nu}(2)_{\max}/(1000\ \text{cm}^{-1}) - 27.52}{-3.182} \qquad (5)$$

Note, the use of wavelengths and wavenumbers in parallel results from the decision to give the original equations for α, β, and π^* from refs 42 and 43. The parameter α was determined according to eq 6:[19]

$$\alpha = \frac{(E_T(30)/(\text{kcal mol}^{-1}) - 14.6(\pi^* - 0.23) - 30.31)}{16.5} \qquad (6)$$

The parameter β was calculated based on the wavenumbers at maximum absorbance of 4-nitroaniline, $\tilde{\nu}(1)_{\max}$, and of *N,N*-diethyl-4-nitroaniline, $\tilde{\nu}(2)_{\max}$.[43]

$$\beta = \frac{1.035\tilde{\nu}(2)_{\max}/(1000\ \text{cm}^{-1}) - \tilde{\nu}(1)_{\max}/(1000\ \text{cm}^{-1}) + 2.64}{2.8} \qquad (7)$$

α, β, and π^* parameters as well as E_T^N of DMSO, THF, MMA, and the ILs are listed in Table 2.

While E_T^N values of [BMIM][PF$_6$], [HMIM]Cl, [HMIM]-[PF$_6$], and [MOIM][BF$_4$] as well as α, β, and π^* parameters of [BMIM][PF$_6$] are in a good agreement with literature values,[44,45] E_T^N values of [BMIM][BF$_4$] differ by up to 10% from the values reported in refs 44 and 45. Because α is closely related to E_T^N (eq 6), α also deviates from literature data: α is about 10% higher

Table 2. E_T^N, π^*, α, and β of Neat Solvents Used for MMA Polymerizations at Ambient Conditions

solvent	E_T^N	π^*	α	β
[EMIM][HexSO$_4$]^a	0.66	0.98	0.65	0.71
[EMIM][OctSO$_4$]	0.63	0.93	0.65	0.77
[BMIM][BF$_4$]^a	0.75	1.04	0.77	0.39
[BMIM][PF$_6$]	0.69	1.02	0.68	0.21
[BMIM][OctSO$_4$]	0.64	0.89	0.69	0.79
[HMIM]Cl^a	0.59	1.02	0.48	0.94
[HMIM]Br^a	0.61	1.09	0.45	0.74
[HMIM][PF$_6$]	0.66	1.02	0.63	0.24
[MOIM][BF$_4$]	0.65	0.98	0.62	0.41
[MOPYR][BF$_4$]	0.60	1.02	0.51	0.44
[OMA][Tf$_2$N]	0.47	0.91	0.35	0.37
DMSO	0.44	1.04	0.18	0.71
THF	0.21	0.59	0.11	0.61
MMA	0.23	0.59	0.16	0.44

[a] Et_3N added.

than the literature value, while π^* and β are in good agreement with previously reported literature data.[44] Deviations in E_T^N and α are probably a consequence of impurities contained in [BMIM][BF$_4$]. It cannot be excluded that the addition of Et_3N to [BMIM][BF$_4$] to scavenge the acid that protonates the phenoxide form of Reichardt's dye and to recover its color is the reason for the differences. However, addition of Et_3N to [HMIM]Cl, [HMIM]Br, and [EMIM][HexSO$_4$] did not lead to significant differences in E_T^N or the Kamlet–Taft parameters compared to literature data.

Although the π^* values of all ILs are rather similar and both anion and cation have an influence on π^*, Table 2 indicates that in particular the size of the anion affects polarity and dipolarizability. The highest π^* values were derived for ILs with rather compact anions, such as halogen anions, hexafluorophosphate, or tetrafluoroborate. The α parameter is also affected by both cation and anion; in contrast, the β parameter is clearly dominated by the nature of the anion. The trends observed in this study are in agreement with previously reported conclusions.[44,46]

In addition to the solvatochromic parameters for pure ILs listed in Table 2, E_T^N, α, β, and π^* were also measured for MMA/IL mixtures at different c_M to enable the prediction of k_p as a function of c_M on the basis of LSER analyses. The solvatochromic parameters of the mixtures are listed in Table 3.

The variation of E_T^N and the Kamlet–Taft parameters with c_M is depicted in Figure 3 for mixtures of MMA with [OMA][Tf$_2$N], [MOPYR][BF$_4$], and [HMIM][PF$_6$]. It is evident that the addition of small amounts of IL to MMA causes an abrupt increase in E_T^N. This observation can be explained by a strong preferential solvation of the dipolar betaine dye by the IL, which is the more polar component of the binary mixture.[29,47] The same behavior is observed for the α parameter: addition of small amounts of IL to MMA results in an abrupt increase of α, whereas α remains almost constant for c_M below 8 mol L^{-1}. Moreover, Figure 3 shows a continuous increase in π^* upon addition of IL, whereas β increases slightly upon addition of small amounts of IL followed by a modest decrease for c_M below 7 mol L^{-1}. This observation, and eq 8 taken from ref 45, suggest that the abrupt increase in E_T^N upon addition of small amounts of IL is mainly the consequence of HBD interactions.

$$E_T^N = 0.01 + 0.36\pi^* + 0.47\alpha \tag{8}$$

Figures 1 and 3 already point out that MMA k_p cannot solely be influenced by E_T^N or α values because MMA k_p increases continuously rather than abruptly with IL content, contrary to the observations for E_T^N and α. Since the IL influence on MMA k_p is too complex to be represented by a single parameter correlation, the linear solvation energy relationship approach was used to interpret MMA k_p enhancement.

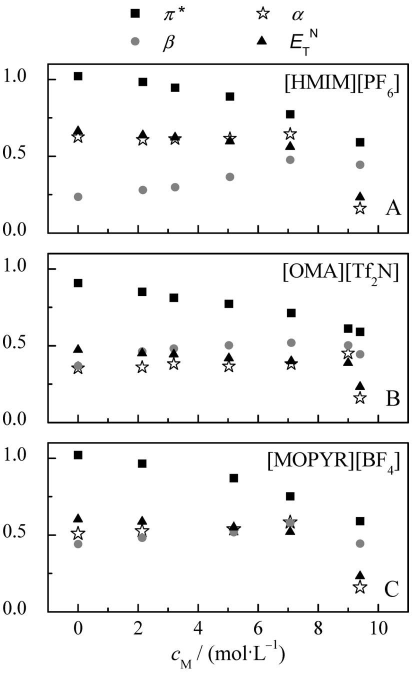

Figure 3. Variation of E_T^N, π^*, α, and β parameters with c_M in MMA mixtures with (A) [HMIM][PF$_6$], (B) [OMA][Tf$_2$N], and (C) [MOPYR][BF$_4$] at ambient conditions (*T*: 23–25 °C).

Table 3. E_T^N, π^*, α, and β of MMA/Solvent Mixtures at Ambient Conditions

solvent	c_M/mol L^{-1}	E_T^N	π^*	α	β
[EMIM][HexSO$_4$]^a	2.14	0.64	0.91	0.68	0.79
[EMIM][OctSO$_4$]	2.15	0.61	0.87	0.66	0.79
[BMIM][BF$_4$]^a	2.11	0.73	1.00	0.77	0.36
[BMIM][PF$_6$]	2.14	0.66	1.00	0.64	0.23
[BMIM][OctSO$_4$]	2.15	0.61	0.83	0.69	0.84
[HMIM]Cl^a	2.13	0.56	0.95	0.49	0.98
[HMIM]Br^a	2.15	0.59	1.00	0.49	0.83
[HMIM][PF$_6$]	2.16	0.64	0.98	0.61	0.28
[HMIM][PF$_6$]	3.23	0.62	0.95	0.61	0.30
[HMIM][PF$_6$]	5.07	0.60	0.89	0.61	0.36
[HMIM][PF$_6$]	7.07	0.56	0.77	0.65	0.48
[MOIM][BF$_4$]	2.14	0.62	0.93	0.62	0.48
[MOPYR][BF$_4$]	2.14	0.59	0.96	0.53	0.48
[MOPYR][BF$_4$]	5.19	0.55	0.87	0.54	0.52
[MOPYR][BF$_4$]	7.07	0.52	0.75	0.58	0.58
[OMA][Tf$_2$N]	2.14	0.45	0.85	0.36	0.46
[OMA][Tf$_2$N]	3.19	0.44	0.81	0.38	0.48
[OMA][Tf$_2$N]	5.03	0.42	0.77	0.37	0.50
[OMA][Tf$_2$N]	7.11	0.40	0.71	0.38	0.52
[OMA][Tf$_2$N]	9.00	0.39	0.61	0.45	0.50
DMSO	2.14	0.43	0.96	0.22	0.75
THF	2.14	0.22	0.59	0.13	0.58

[a] Et_3N added.

To correlate the IL influence with the Kamlet–Taft parameters, a multiparameter analysis was applied, more specifically, the linear solvation energy relationship (LSER) of Kamlet and Taft. The LSER approach is used to identify and to quantify multiple solvent effects on MMA k_p. Here, LSER is applied to $k_p/k_{p,\mathrm{bulk}}$ data:

$$\ln(k_p/k_{p,\,\mathrm{bulk}}) = \ln(k_p/k_{p,\,\mathrm{bulk}})^0 + s\pi^* + \mathrm{a}\alpha + \mathrm{b}\beta \tag{9}$$

where $\ln(k_p/k_{p,\mathrm{bulk}})^0$ refers to a theoretical value in an inert solvent.[19] As the π^* values for all ILs are rather similar, the polarizability correction term δ from eq 1 is not considered. The LSER analyses were carried out using OriginPro 8 or Microsoft Excel 2003 applying multiple linear regression analyses

Table 4. LSER Coefficients Obtained by Multiple Linear Regression Analyses[a]

LSER	$\ln(k_p/k_{p,\mathrm{bulk}})^0$	*s*	*a*	*b*	*N*	R^2	*S*
1	−1.74 (0.55)	2.34 (0.51)	0.37 (0.25)	0.41 (0.13)	11	0.80	0.098
2	−1.89 (0.54)	2.60 (0.53)	0.28 (0.26)	0.53 (0.13)	11	0.81	0.095
1a	−1.46 (0.56)	2.30 (0.55)		0.38 (0.13)	11	0.74	0.11
2a	−1.75 (0.54)	2.64 (0.53)		0.51 (0.13)	11	0.78	0.096
3	−1.27 (0.20)	1.72 (0.25)	0.63 (0.18)	0.37 (0.14)	14	0.94	0.11
4	−1.43 (0.23)	1.94 (0.29)	0.62 (0.19)	0.44 (0.13)	14	0.94	0.11
5	−1.59 (0.053)	2.68 (0.070)			5	0.99	0.014
6	−1.42 (0.20)	2.31 (0.24)			5	0.97	0.076

[a] The values in parentheses are standard errors of the coefficients. *N*: number of data sets, R^2: coefficient of determination, *S*: standard error of the estimate. Details for all LSER analyses are given in the text.

on correlations of experimental $k_p/k_{p,\mathrm{bulk}}$ values with α, β, and π^* (eq 9). The resulting coefficients *a*, *b*, and *s* for MMA polymerizations in ILs at $c_M = 2$ mol L^{-1} based on solvent parameters of the neat ILs from Table 2 are given as LSER 1 in Table 4. The standard error of each coefficient (given in parentheses), number of data sets used in LSER, *N*, coefficient of determination, R^2, and standard error of estimate, *S*, are also listed in Table 4.

The same set of MMA k_p values obtained in ILs at $c_M = 2$ mol L^{-1} were also correlated with solvent parameters of MMA/IL mixtures for $c_M = 2$ mol L^{-1} (Table 3), resulting in LSER 2.

Experimentally obtained MMA $\ln(k_p/k_{p,\mathrm{bulk}})$ values vs those calculated from LSER 1 and 2 are depicted in Figure 4A. The full line represents a linear fit of the data points. For both analyses no differences can be seen. The positive and negative deviations of the experimental data from the predictions appear to be random; e.g., [HMIM]Cl and [HMIM]Br having the strongest influence on k_p show a positive deviation and a negative deviation from the fit, respectively. Interestingly, the coefficients of LSER 1 and 2 are very similar despite LSER 1 is based on pure IL parameters accounting for IL interactions only and LSER 2 is based on parameters for MMA/IL mixtures accounting for interactions with monomer and IL. All coefficients from LSER 1 and 2 have a positive sign, suggesting that all the interactions represented by the corresponding parameters contribute to a stabilization of the transition state structure of the propagation step and resulting in a k_p increase.[29] However, due to a high standard error, the influence of the α parameter cannot be determined precisely.[25,27,28] Furthermore, relative contributions of α, β, and π^* to the LSER are significantly different. The percentage contributions of each parameter to the LSERs are calculated from the coefficients *s*, *a*, and *b*. The relative contributions listed in Table 5 indicate the importance of the π^* parameter, which accounts for polarity/polarizability and the ability to undergo EPA interactions, for MMA propagation kinetics. The HBD and HBA/EPD ability of the ILs represented by the α and β parameters, respectively, have a significantly lower influence on MMA k_p.

LSER 1 clearly suggests that the transition state is better stabilized than the reactants and that this is primarily a consequence of solute−solvent interactions expressed by parameter π^*. The result obtained from LSER 2 is almost identical to LSER 1. This may be explained by the fact that addition of small amounts of MMA (2 mol L^{-1}) does not result in a significant change in LSER parameters of the ILs (Figure 3 and Tables 2 and 3). This was also reported by Mellein at al.,[47] who determined LSER parameters for numerous IL/organic solvents mixtures.

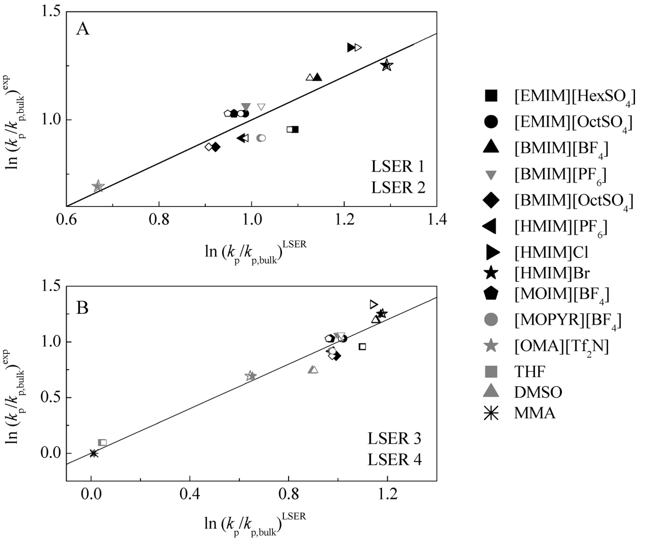

Figure 4. Experimentally obtained $\ln(k_p/k_{p,\mathrm{bulk}})^{\mathrm{exp}}$ vs $\ln(k_p/k_{p,\mathrm{bulk}})^{\mathrm{LSER}}$ predicted by LSERs. Lines represent LSER fits. Filled symbols refer to solvatochromic parameters for neat solvents and open symbols to parameters for MMA/solvent mixtures. Coefficients of LSER 1−4 are contained in Table 4.

Table 5. Relative Contributions (*P*) of Kamlet−Taft's Solvatochromic Parameters to the LSERs, e.g., $P_{\pi^*} = s/(a + b + s)$

LSER	P_{π^*}	P_α	P_β
1	0.75	0.12	0.13
2	0.76	0.08	0.16
1a	0.86	n.a.[a]	0.14
2a	0.84	n.a.[a]	0.16
3	0.63	0.23	0.14
4	0.65	0.21	0.15

[a] n.a.: not applicable since LSER without α.

Therefore, the result of LSER 2 is still mainly governed by IL properties.

Since the standard error of the *a* coefficient is rather high indicating that α is not well-determined, it was tested whether the data may be represented by two-parameter correlations excluding the α parameter. The results are presented in Table 4 as LSERs 1a and 2a. The advantage of using LSERs 1a and 2a to predict MMA k_p values is that only two parameters are required, while LSERs 1 and 2 include all three parameters. A disadvantage of using LSERs 1a and 2a instead of LSERs 1 and 2 is a lower accuracy, indicated by lower values of R^2 in case of LSERs 1a and 2a.

As all ILs investigated have a very narrow range of π^* values, it appeared important to extend the range of π^* values and to confirm the importance of π^* for MMA propagation kinetics by including some other solvents in the analyses. Therefore, the LSER was extended for MMA k_p values determined in THF,[38] DMSO, and for MMA bulk. Addition of these data to LSER 1 resulted in LSER 3. Including these systems to LSER 2 yielded LSER 4. The coefficients and statistics of LSERs 3 and 4 are given in Table 4. Because of the small number of additional data, we refrained from including the δ parameter into the analysis.

Of course, an extension of the range of values for the solvatochromic parameters including THF, DMSO, and MMA into the data set also extended the k_p range significantly, contributing to an improvement of the fits. Statistical data from Table 4 show that all parameters are significant. Even with these improvements, relative contributions of π^* (Table 5) remain distinctively higher than the contributions of the other parameters. The α parameter in LSERs 3 and 4 is now determined since the standard error of α is significantly lower than for LSERs

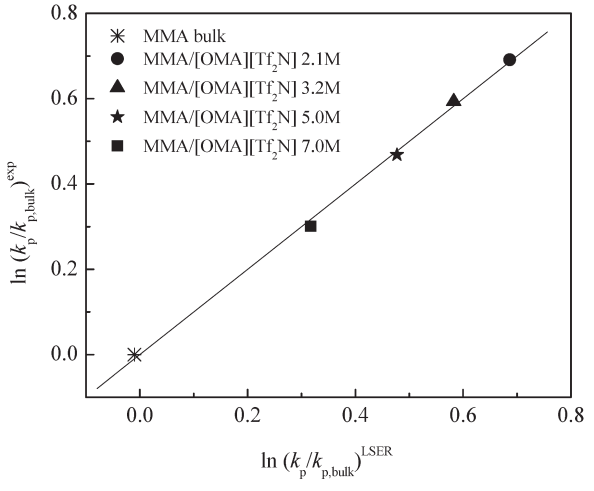

Figure 5. Experimentally obtained $\ln(k_p/k_{p,\mathrm{bulk}})^{\mathrm{exp}}$ values for MMA polymerizations in [OMA][Tf$_2$N] vs $\ln(k_p/k_{p,\mathrm{bulk}})^{\mathrm{LSER}}$ calculated from LSER 5.

1 and 2. The contribution of α (P_α) is around 20% (Table 5). The finding that α is not precisely determined (LSER 1 and 2) or is only of minor importance (LSER 3 and 4) is in accordance with previous findings from IR spectroscopy. IR spectra of MMA/IL mixtures did not show significant contributions from H-bonding.[14]

A simplification of LSERs 3 and 4 to two-parameter (including π^* and α, or π^* and β) and one-parameter equations (using only π^*) resulted in relatively successful correlations, but R^2 being significantly lower than for the three-parameter equation. The importance of π^* for the IL influence on MMA k_p is reflected by the fact that all LSER analyses including π^* yield a reasonable well description of the IL influence on k_p. The introduction of the δ term would probably somewhat improve the fitting precision but at the same time would result in a more complex LSER analysis.

Since both LSERs obtained with parameters for neat solvents and MMA/solvent mixtures resulted in fits of similar high quality, LSERs obtained on the basis of solvatochromic parameters for neat ILs should be advantageous for the prediction of MMA k_p, as literature data for pure ILs may be used. Contrary, finding appropriate data published for MMA/IL mixtures is rather unlikely.

LSER analysis was also applied to predict MMA k_p values obtained for different c_M concentrations in a given IL. Correlation of MMA k_p determined for MMA/[OMA][Tf$_2$N] mixtures of different c_M and MMA k_p bulk with corresponding solvatochromic parameters at identical c_M resulted in an LSER of excellent precession. However, high standard errors of coefficients a and b in this correlation render the parameters α and β statistically insignificant. Analyses employing a reduced number of parameters are only successful if the π^* parameter is considered. The resulting LSER 5 is given in Table 4. In Figure 5 experimental $\ln(k_p/k_{p,\mathrm{bulk}})^{\mathrm{exp}}$ values for MMA polymerizations in [OMA][Tf$_2$N] were plotted vs $\ln(k_p/k_{p,\mathrm{bulk}})^{\mathrm{LSER}}$ calculated from LSER 5.

LSER 5 gives an excellent and very simple tool for the prediction of MMA k_p at different c_M in [OMA][Tf$_2$N]. The resulting correlation with a single parameter in LSER 5 is not surprising considering the fact that α and β parameters remain almost the same over the entire range of different c_M in MMA/[OMA][Tf$_2$N] mixtures (Figure 3).

To confirm that the results obtained by LSER 5 are not incidental and a similar relationship can be obtained for other ILs, the correlation of MMA k_p with Kamlet–Taft solvatochromic parameters at different c_M via LSER was also employed for MMA/[HMIM][PF$_6$] mixtures. [HMIM][PF$_6$] was randomly chosen among the ILs showing homogeneous reaction mixtures before and after PLP. As for polymerizations in [OMA][Tf$_2$N] a three-parameter LSER resulted in coefficients of α and β with high standard deviation. The correlation obtained on the basis of the π^* parameter only was again successful. The one-parameter LSER 6 and its statistical data are listed in Table 4.

Conclusions

Pulsed laser initiated polymerizations and subsequent polymer molecular weight analyses showed a strong influence of the IL on propagation rate coefficients in MMA radical polymerizations. In an effort to predict the influence of an IL on MMA k_p, multiple linear solvation energy relationship analyses were applied to correlate the IL-induced variation of MMA k_p to the Kamlet–Taft parameters of the neat ILs and of MMA/IL mixtures. It is shown that a wide range of data for ILs and organic solvents such as DMSO or THF may be represented by a single LSER fit. The LSER coefficients of the Kamlet–Taft parameters indicate that dipolarity/polarizability and electron pair accepting ability, which is accounted for by π^*, determine to a large extent how much k_p is varied due to the presence of a solvent. The contributions from the H-bond accepting and the electron pair donating ability of ILs, as given by β, are of significantly less importance. The H-bond donating ability of the ILs, associated with the α parameter, has a minor influence on MMA k_p. Further, it was shown that the LSER analyses may be carried out with Kamlet–Taft parameters of neat ILs. Thus, k_p data for MMA polymerizations in ILs may be estimated from tabulated Kamlet–Taft parameters of neat ILs.

Acknowledgment. A.J. and S.B. gratefully acknowledge financial support by University of Potsdam in the framework of the Graduate School on Green Chemistry. Experimental assistance with the operation of the laser and UV measurements by Christian Brendler and Diana Hill is acknowledged. N.G. thanks the Spanish Ministry of Science and Technology for funding (Programma "Ramón y Cajal" and MAT2008-06725-C03-01).

References and Notes

(1) Wasserscheid, P.; Welton, T. *Ionic Liquids in Synthesis*; WILEY-VCH Verlag Gmbh & Co.: Berlin, 2008.
(2) Kubisa, P. *Prog. Polym. Sci.* **2004**, *29*, 3.
(3) Kubisa, P. *J. Polym. Sci., Part A: Polym. Chem.* **2005**, *43*, 4675.
(4) *Ionic liquids in Polymer Systems: Solvents, Additives, and Novel Applications*; Brazel, C. S., Rogers, R. D., Eds.; ACS Symposium Series 913; American Chemical Society: Washington, DC, 2005.
(5) Biedron, T.; Kubisa, P. *J. Polym. Sci., Part A: Polym. Chem.* **2005**, *43*, 3454.
(6) Ryan, J.; Aldabbagh, F.; Zetterlund, P. B.; Yamada, B. *Macromol. Rapid Commun.* **2004**, *25*, 930.
(7) Lu, J.; Yan, F.; Texter, J. *Prog. Polym. Sci.* **2009**, *34*, 431.
(8) Ueki, T.; Watanabe, M. *Macromolecules* **2008**, *41*, 3739.
(9) Hong, K.; Zhang, H.; Mays, J. W.; Visser, A. E.; Brazel, C. S.; Holbrey, J. D.; Reichert, W. M.; Rogers, R. D. *Chem. Commun.* **2002**, 1368.
(10) Strehmel, V.; Laschewsky, A.; Wetzel, H.; Görnitz, E. *Macromolecules* **2006**, *39*, 923.
(11) Harrisson, S.; Mackenzie, S. R.; Haddleton, D. M. *Macromolecules* **2003**, *36*, 5072.
(12) Woecht, I.; Schmidt-Naake, G.; Beuermann, S.; Buback, M.; García, N. *J. Polym. Sci., Part A: Polym. Chem.* **2008**, *46*, 1460.
(13) Beuermann, S. *Macromol. Rapid Commun.* **2009**, *30*, 1066.
(14) Jeličić, A.; Beuermann, S.; García, N. *Macromolecules* **2009**, *42*, 5062.
(15) Zhang, H.; Hong, K. L.; Mays, J. W. *Macromolecules* **2002**, *35*, 5738.
(16) Zhang, H.; Hong, K.; Jablonsky, M.; Mays, J. W. *Chem. Commun.* **2003**, 1356.
(17) Strehmel, V.; Laschewsky, A.; Wetzel, H. *e-Polym.* **2006**, no. 011.

(18) Li, J.; Zhang, J.; Liu, Z. *J. Polym. Sci., Part A: Polym. Chem.* **2006**, *44*, 4420.
(19) Kamlet, M. J.; Abboud, J.-L. M.; Abraham, M. H.; Taft, R. W. *J. Org. Chem.* **1983**, *48*, 2877.
(20) Taft, R. W.; Abboud, J.-L. M.; Kamlet, M. J. *J. Am. Chem. Soc.* **1981**, *103*, 1080.
(21) Crowhurst, L.; Falcone, R.; Lancaster, N. L.; Llopis-Mestre, V.; Welton, T. *J. Org. Chem.* **2006**, *71*, 8847.
(22) García-Río, L.; Leis, J. R.; Iglesias, E. *J. Org. Chem.* **1997**, *62*, 4712.
(23) Adam, C.; García-Río, L.; Godoy, A.; Ramón Leis, J. *Green Chem.* **2006**, *8*, 596.
(24) Ranieri, G.; Hallett, J. P.; Welton, T. *Ind. Eng. Chem. Res.* **2008**, *47*, 638.
(25) Marinković, A. D.; Drmanić, S. Ž.; Jovanović, B. Ž.; Mišić-Vuković, M. *J. Serb. Chem. Soc.* **2005**, *70*, 557.
(26) Marcus, Y. *J. Solution Chem.* **1991**, *20*, 929.
(27) Nikolić, J. B.; Ušćumlić, G. S. *J. Serb. Chem. Soc.* **2007**, *72*, 1217.
(28) Nikolić, J. B.; Ušćumlić, G. S.; Krstić, V. V. *J. Serb. Chem. Soc.* **2004**, *69*, 601.
(29) *Solvents and Solvent Effects in Organic Chemistry*, 2nd ed.; Reichardt, C., Ed.; Wiley-VCH: Weinheim, 1990.
(30) Czerwinski, W. K. *Macromolecules* **1995**, *28*, 5405.
(31) García, N.; Tiemblo, P.; Guzmán, J. *Macromolecules* **2007**, *40*, 4802.
(32) Harrod, W. B.; Pienta, N. J. *J. Phys. Org. Chem.* **1990**, *3*, 534.
(33) Olaj, O. F.; Bitai, I.; Hinkelmann, F. *Makromol. Chem.* **1987**, *188*, 1689.
(34) Buback, M.; Gilbert, R. G.; Russell, G. T.; Hill, D. J. T.; O'Driscoll, K. F.; Shen, J.; Winnik, M. A. *J. Polym. Sci., Part A: Polym. Chem.* **1992**, *30*, 851.
(35) Beuermann, S.; Buback, M.; Davis, T. P.; Gilbert, R. G.; Hutchinson, R. A.; Olaj, O. F.; Russell, G. T.; Schweer, J.; van Herk, A. M. *Macromol. Chem. Phys.* **1997**, *198*, 1545.
(36) Hutchinson, R. A.; Aronson, M. T.; Richards, J. R. *Macromolecules* **1993**, *26*, 6410.
(37) Buback, M.; Gilbert, R. G.; Hutchinson, R. A.; Klumperman, B.; Kuchta, F.-D.; Manders, B. G.; O'Driscoll, K. F.; Russell, G. T.; Schweer, J. *Macromol. Chem. Phys.* **1995**, *196*, 3267.
(38) Beuermann, S.; García, N. *Macromolecules* **2004**, *37*, 3018.
(39) Beuermann, S.; Buback, M.; Kuchta, F.-D.; Schmaltz, C. *Macromol. Chem. Phys.* **1998**, *199*, 1209.
(40) Beuermann, S.; Buback, M.; El Rezzi, V.; Jürgens, M.; Nelke, D. *Macromol. Chem. Phys.* **2004**, *205*, 876.
(41) Reichardt, C. *Chem. Rev.* **1994**, *94*, 2319.
(42) Kamlet, M. J.; Abboud, J. L.; Taft, R. W. *J. Am. Chem. Soc.* **1977**, *99*, 6027.
(43) Kamlet, M. J.; Taft, R. W. *J. Am. Chem. Soc.* **1976**, *98*, 377.
(44) Crowhurst, L.; Mawdsley, P. R.; Perez-Arlandis, J. M.; Salter, P. A.; Welton, T. *Phys. Chem. Chem. Phys.* **2003**, *5*, 2790.
(45) Reichardt, C. *Green Chem.* **2005**, *7*, 339.
(46) Lee, J.-M.; Ruckes, S.; Prausnitz, J. M. *J. Phys. Chem. B* **2008**, *112*, 1473.
(47) Mellein, B. R.; Aki, S. N. V. K.; Ladewski, R. L.; Brennecke, J. F. *J. Phys. Chem. B* **2007**, *111*, 131.